Pergamon

Cement and Concrete Research 29 (1999) 297–302

CEMENT AND CONCRETE RESEARCH

Fly ash from cellulose industry as secondary raw material in autoclaved aerated concrete

André Hauser [a], Urs Eggenberger [a,*], Thomas Mumenthaler [b]

[a]Mineralogisch-Petrographisches Institut, Baltzerstr. 1, 3012 Bern, Switzerland
[b]ZZ Ziegeleien, Giesshübelstr. 45, 8045 Zürich, Switzerland

Manuscript received 3 October 1997; accepted manuscript 2 November 1998

Abstract

Because fly ash from cellulose industries contains considerable amounts of free lime and sulfate, they are potential secondary raw materials for the production of autoclaved aerated concrete. Laboratory experiments were performed by replacing lime and sulfate in conventional autoclaved aerated concrete mixtures by fly ash. Compared to a reference series, samples with even higher compressive strength could be produced with lime-sulfate ash. At higher proportions of fly ash, the formation of calcium silicate hydrate phases is delayed and the presence of unreacted portlandite and newly formed scawtite produce a drop in strength and an increase in shrinkage. Low strength resulted by using Al-bearing ash with a lower amount of free CaO, which makes this type of ash not applicable in practice. © 1999 Elsevier Science Ltd. All rights reserved.

Keywords: Fly ash; Thermal treatment; Concrete; Sulfate

Autoclaved aerated concrete (AAC) usually is made from quartz-rich sand, lime, cement, and calcium sulfate with traces of aluminium powder as pore-forming agent. These components are mixed with high amounts of water and molded to produce a cellular green body by H_2-gas generation at atmospheric pressure, and then autoclaved at 200°C under saturated steam pressure for several hours. Calcium silicate hydrate (CSH) phases are formed from reactions between silicates and CaO of the bonding agent.

Generally, the physical properties of autoclaved aerated concrete are determined by its structure, mineralogical composition, and texture. Although the structure can be controlled up to a certain extent by addition of pore-forming agents such as Al powder and water, mineralogical composition and texture depend strongly on composition and reactivity of the raw materials. For these reasons the influence of new raw materials on phase formation must be studied carefully.

The influence of alternative SiO_2 sources, as well as various Al compounds, on phase formation under hydrothermal conditions was studied by many authors [1–13]. Pure substances and different commercial products including waste materials such as fly ash and slag from power plants, bricks, and tiles were considered as sources for SiO_2 and Al_2O_3. In contrast, different types and sources of CaO and $CaSO_4$ and their behavior in the hydrothermal process were rarely investigated [14]).

In this study, AAC was produced using ash as a raw material. Experiments on a laboratory scale were carried out with mixtures in which lime and sulfate are totally substituted by ash. The goal of these series was to substitute primary raw materials as well as to optimize strength. Furthermore, samples were examined by various mineralogical and chemical methods to establish relationships between the mineralogical composition and the physical properties.

1. Materials

Fly ash from cellulose industries are fine-grained, lime- and sulfate-containing waste products. The characterization of the ashes including chemical, mineralogical, and physical properties as well as results from experiments with hydrothermally treated ash were reported previously [15]. Two principal types of fly ash, originating from two waste combustion stages, can be distinguished. Lime-sulfate ashes are mainly composed of free lime and anhydrite, whereas Al-bearing ashes contain less lime and sulfate but considerable amounts of low reactive calcium silicates and highly reactive calcium aluminates (Table 1). Minor phases include low crystalline calcite, portlandite, hydroxyl-ellestadite, and quartz. Due to coatings on particle surfaces and elevated

---

* Corresponding author. Tel.: 41-31-631-4843.

0008-8846/99/$–see front matter © 1999 Elsevier Science Ltd. All rights reserved.
PII: S0008-8846(98)00207-5

Table 1
Data on the applied fly ashes from cellulose industry

Type	Av. CaO	SiO_2tot.	Al_2O_3tot.	$CaSO_4$tot.	Na_2O
Lime-sulfate ash	43.9	0.42	0.26	31.0	2.34
Al-bearing ash	24.4	14.51	9.30	10.7	0.44

The amounts of available lime (Av. CaO), total SiO_2 (SiO_2tot.), total Al_2O_3 (Al_2O_3tot.), total SO_3 expressed as $CaSO_4$ ($CaSO_4$tot.) and Na_2O are given in wt%.

contents of sulfate and alkalis, the reactivity of CaO in the ash is significantly lower compared to commercial lime.

2. Experimental procedures and analyzing methods

2.1. Sample preparation

Based on a dry commercial mixture of sand (60 wt%), lime (11 wt%), sulfate (4 wt%), and cement (25 wt%), an analogous reference mixture (2500g) was produced. Al powder was used as pore-forming agent (0.06 wt%). Mixtures of the reference series were obtained by varying the lime-to-sand ratio while sulfate and cement contents were held constant in all samples.

In the series with ash, commercial lime and sulfate were entirely substituted by lime-sulfate ash and Al-bearing ash, respectively. Variations in the compositions were obtained by adjusting the ash-to-sand ratio at a constant cement content.

The variations of the lime-to-sand and ash-to-sand ratio, respectively, as well as their relationship to the lime-to-silica ratio (bulk C/S ratio) are shown in Fig. 1. The lime-to-silica ratio is calculated as follows: CaO includes total CaO from cement and available lime from ash and commercial lime, whereas SiO_2 represents total SiO_2 from cement as well as quartz from sand and Al-bearing ash. The sulfate content is directly linked with the sulfate content of the ash and therefore increases with increasing bulk C/S ratio. Other important factors are the amount of available Al_2O_3 as well as the content of available alkalis that are contributed by all ashes.

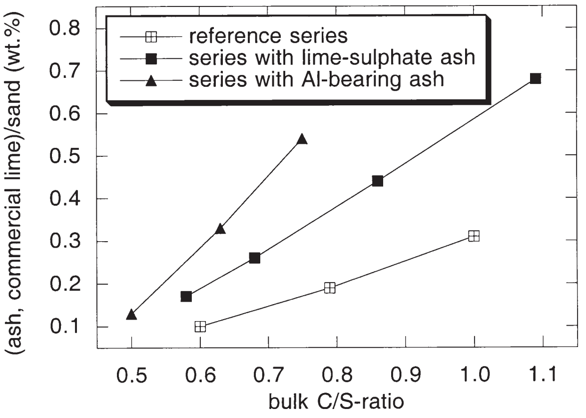

Fig. 1. Composition of the dry raw mixtures. Variations of the bulk C/S ratio were achieved by different lime-to-sand and ash-to-sand ratios, respectively.

The pastes were produced by mixing with warm water (60°C). The water-to-solid ratio was adjusted to obtain pastes of workable viscosity and was balanced with the amount of added Al powder (0.04–0.06 wt%) to control porosity. The pastes were mixed in a laboratory stirrer and cast into steel molds with a volume of 5000 mL. After a reaction time of about 4 h at atmospheric conditions, the samples were cured in an industrial autoclave for 6 h at 200°C.

2.2. Analyzing methods

Compressive strength was measured using three 120-mm cubes, which were dried at 80°C for 24 h. The flatness of the load-bearing surfaces was adjusted by grinding. Force was applied perpendicular to the direction of the rising mass during manufacturing. Moisture content and bulk density were determined after drying at 160°C for 24 h. The compressive strength was normalized to a moisture content of 10 wt% after the relation reported by Aroni et al. [16], which represents an average of the relations shown by other authors [17–19] (Table 2).

Because it was not possible to keep bulk density constant for all samples, the measured compressive strength was normalized to an intermediate bulk density of 650 kg/m^3 after Eq. (1):

$$\text{Compressive strength} = k(\text{bulk density})^2, \tag{1}$$

where k represents a coefficient for the compressive strength, which is independent of bulk density [20]. Shrinkage was obtained by measuring the relative length change during moisture movement of water saturated prisms and subsequent drying at 20°C and 45% relative humidity for at least 1 month. The data of the physical properties represent average values obtained by measurements on two or three specimens. Error bars indicate extreme values.

For the mineralogical investigations the autoclaved material was dried at 50°C and ground. X-ray diffraction (XRD) analyses were carried out on a Philips PW1800 diffractometer equipped with an automatic divergence slit using CuKα radiation. The internal standard method using LiF was applied for semiquantitative measurements. The solubility of SiO_2 in hot (boiling) and cold (5°C) HCl was determined [21,22]. Residual portlandite was analyzed by the sugar method [23].

Table 2
Correction factors of the compressive strength at different moisture contents after Aroni et al. [16]

Moisture (wt%)	0.00	0.15	3.00	6.00	10.00	20.00	30.00	40.00	50.00
Correction factor	1.31	1.30	1.20	1.10	1.00	0.95	0.93	0.92	0.92

Intermediate values were calculated by interpolation.

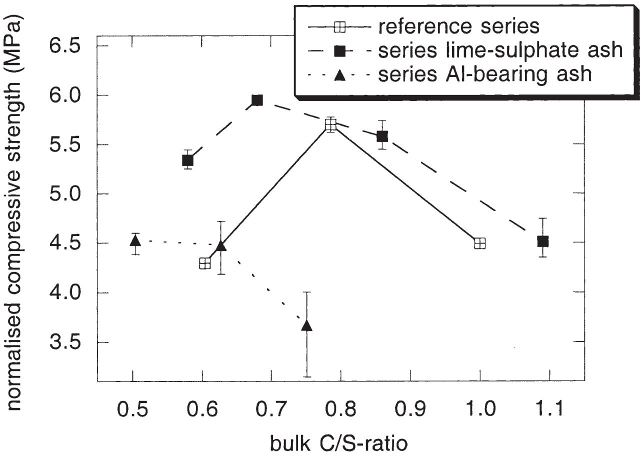

Fig. 2. Compressive strength normalized to a bulk density of 650 kg/m^3 and 10 wt% moisture content. Bars represent minimum and maximum values.

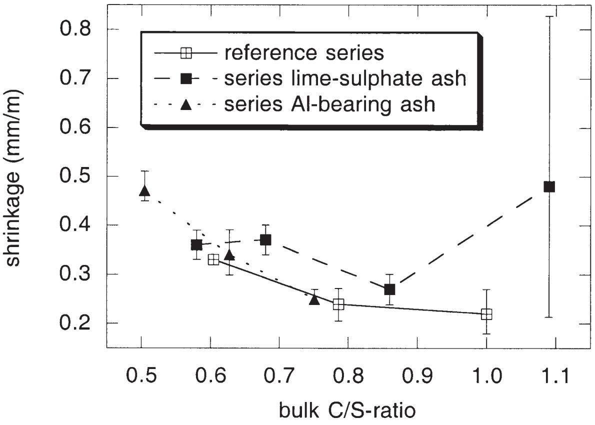

Fig. 3. Shrinkage, defined as length change between 5 days of immersion in water and equilibration at 20°C and 45% relative humidity.

3. Results

3.1. Compressive strength and shrinkage

Normalized values for the compressive strength are plotted against the bulk C/S ratio (Fig. 2). The reference series and the series with lime-sulfate ash have maximum strengths at bulk C/S ratios in the range from 0.6 to 0.8. The highest compressive strengths are obtained by the series with lime-sulfate ash followed by the reference series. Low strength is obtained by the series with Al-bearing ash, which decreases with increasing proportions of ash.

Shrinkage, defined as relative length change between the water-saturated and subsequent dried specimen, generally decreases with increasing bulk C/S ratio (Fig. 3). At lower to intermediate bulk C/S ratios, shrinkage of the series with ash are comparable to the reference series. At higher bulk C/S ratios, samples of the series with lime-sulfate ash show more shrinkage.

3.2. XRD analysis

Semiquantitative concentrations of tobermorite (d = 1.13 nm), xonotlite (0.70 nm), hydrogarnet (0.51 nm), portlandite (0.49 nm), and scawtite (0.46 nm) given as XRD peak intensities relative to an internal standard are shown in Fig. 4a. Tobermorite was detected in all samples. In the reference series and series with Al-bearing ashes, peak intensities for tobermorite, d(002) = 1.13 nm, increase with increasing bulk C/S ratio. The tobermorite intensity of series with lime-sulfate ash is almost constant. Hydrogarnet with a composition near C_3ASH_4 occurs in all series, decreasing with increasing bulk C/S ratio. Xonotlite was only observed at high bulk C/S ratios of the reference series. Scawtite is present at high bulk C/S ratios of series with ashes.

3.3. Soluble SiO_2

Solubility of SiO_2 in HCl (Fig. 4b) can be correlated to the crystallinity of CSH (Fig. 4a). SiO_2 soluble in hot HCl corresponds to the total CSH. Weakly crystallized tobermorite, and semicrystalline and nearly amorphous CSH are only soluble in cold HCl. The difference between hot and cold extracts is related to well-crystallized CSH phases such as tobermorite and xonotlite [9]. In the reference series, the soluble (hot and cold) as well as the insoluble amount of SiO_2 increases with increasing bulk C/S ratio, indicating an increase of more stable CSH phases with increasing bulk C/S ratio. In contrast, in both series with ash, the amount of soluble SiO_2 in cold HCl increases more rapidly than in hot HCl at higher bulk C/S ratios, resulting in a decrease in the amount of insoluble SiO_2 at higher bulk C/S ratios.

4. Discussion

4.1. Phase formation of AAC

During autoclaving, poorly crystalline primary phases rich in Ca are formed first (polymerization state), due to the high concentration of $Ca(OH)_2$ in the solution with respect to silica, followed by subsequent reactions with dissolved silica forming CSH toward lower C/S ratios (CSH I $>$ CSH II $>$ tobermorite) and a higher degree of crystallinity [24]. The phase formation is kinetically controlled and influenced by a number of parameters. The most important for the following discussion are:

- Raeni [14] studied the influence of lime with different reactivities and found higher amounts of semicrystalline phases by using lime with lower specific surface area.
- The role of sulfate is not yet completely explained. It was observed that sulfate accelerates the formation of tobermorite and favored its crystallinity [25]. Investigations of Sauman [26] indicate that these effects are more pronounced if Al is simultaneously available. In pure lime-silica mixtures, sulfate retards the hydrothermal reaction sequence [3].
- The presence of elevated amounts of available sodium accelerates the formation of semicrystalline CSH but

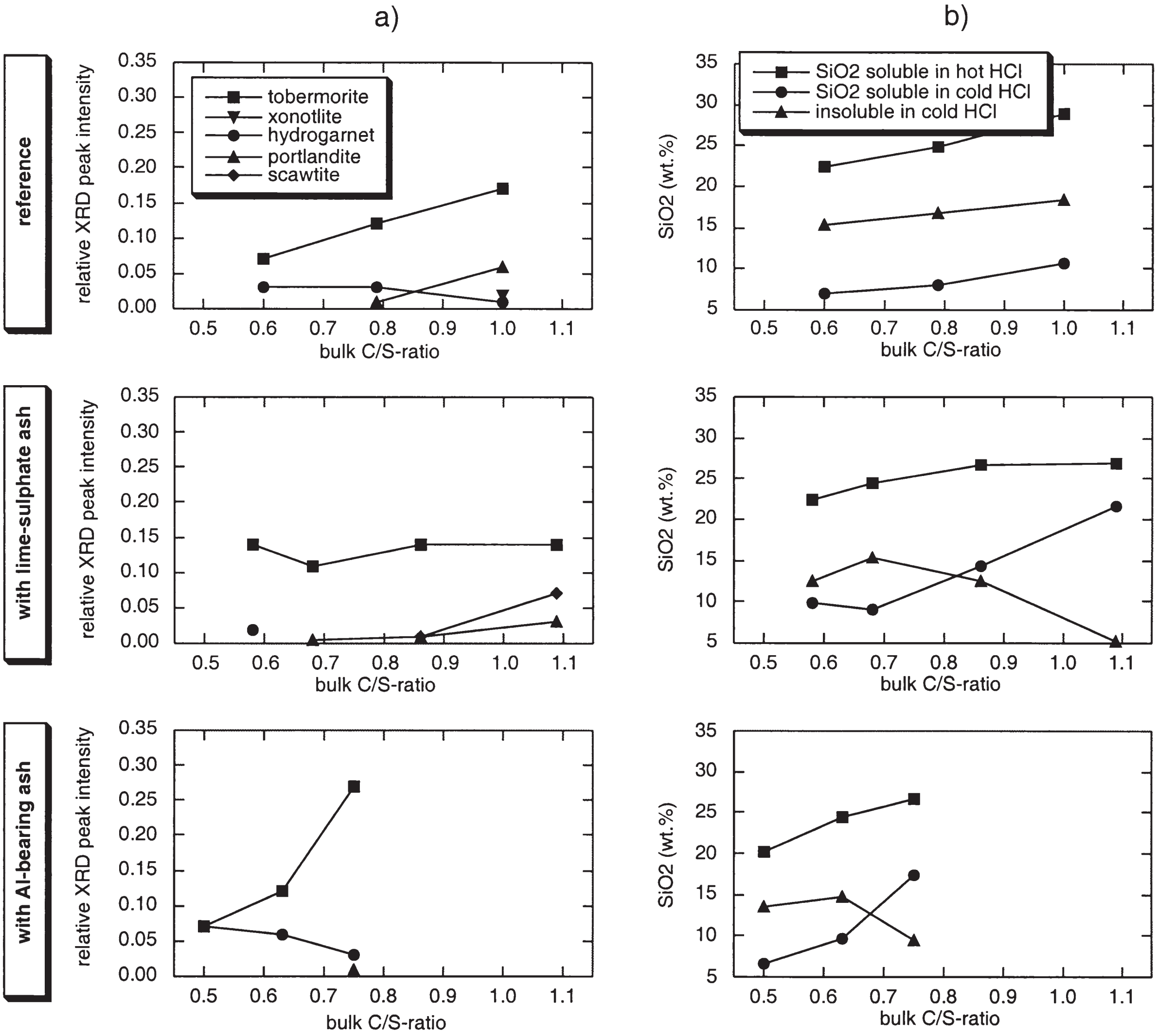

Fig. 4. Results from mineralogical investigations on autoclaved aerated concrete plotted against the bulk C/S ratio for each series. *(a)* Relative XRD peak intensities. *(b)* SiO_2 soluble in hot and cold HCl, respectively, as well as the difference between hot and cold extracts.

suppresses the subsequent formation of tobermorite [27–31].

- Many authors reported that Al_2O_3 favors the formation of tobermorite and raises the crystallinity [8,10,31,32]. Other authors pointed out that Al_2O_3 enhances crystallinity in the crystallographic c-direction of the CSH structure to a greater extent than within the ab-plane [32–34]. Crystallinity within the ab-plane reflects the degree of polymerization of the silicate structures, which is measured by the solubility of SiO_2 in HCl. Furthermore, Al itself is suggested to retard reaction rates at high bulk C/S ratios [30,31,35–37]. Similar effects were shown by experiments of Gabrovsek et al. [38,39]. They investigated the influence of Al_2O_3 and Al_2O_3 + Na_2O and found that the degree of condensation of the silicate anions in tobermorite was significantly lowered by both.

At very high bulk C/S ratios, portlandite and scawtite may form. The formation of scawtite is favored by the presence of $CaCO_3$, which was reported in a number of studies [7,40–44], and there is no evidence that CO_2 from the atmosphere or from water may be the source of CO_2 to form scawtite [7,42,45].

4.2. Reference series: phase formation and physical parameters

In the reference series, a high reaction rate is demonstrated by the high amounts of well-crystallized tobermorite, low proportions of poorly crystalline CSH, as well as the presence of xonotlite at high bulk C/S ratios. Although the total amount of CSH represented by the SiO_2 soluble in hot HCl increases within the given range of bulk C/S ratio, slightly increasing proportions of SiO_2 soluble in cold HCl and unreacted portlandite indicate that the reaction sequence remains increasingly incomplete with increasing bulk C/S ratio.

The behavior of the compressive strength is strongly related to the mineralogical properties of AAC. At a bulk C/S ratio below 0.8, increasing strength is correlated with increasing total amount of CSH [32,46,47]. At a bulk C/S ratio above 0.8, the ratio of sand to binding agent no longer is ideal, thus having a negative influence on strength and promoting the formation of xonotlite [11,47,48]. Decreasing shrinkage with increasing bulk C/S ratio is explained by increasing degree of crystallinity of the CSH phases [1,49].

4.3. Series with lime-sulfate ash: phase formation and physical parameters

The composition of the CSH phases in autoclaved samples of the series with lime-sulfate ash shows significant differences compared to the reference series. Although peak intensities for tobermorite remain approximately constant with increasing bulk C/S ratio, the proportion of semicrystalline CSH increases as shown by the solubility of SiO_2 in cold HCl. The absence of hydrogarnet at higher bulk C/S ratios might be a further indication that aluminium sources such as feldspar and clay minerals are consumed only to a minor extent. This indicates incomplete reaction sequences caused by retarding effects of the added lime-sulfate ash.

By analogy to Raeni [14], the low reactive CaO of the lime-sulfate ash favors the initial formation of Ca-poorer CSH, which subsequently reacts more sluggishly with silica [2,5,50,51]. Elevated amounts of available sodium in the series with lime-sulfate ash (Na_2O: 1.53 wt%) in comparison to the reference series (1.16 wt%), accelerates the formation of semicrystalline CSH and suppresses the formation of tobermorite [27–31]. The predominance of semicrystalline CSH might be due to the initial formation of Ca-poorer CSH [52] and their retarding effects on the reaction sequence. Mixtures of the series with lime-sulfate ashes have high sulfate concentrations but low amounts of Al_2O_3. The retardation effect of sulfate on the reaction sequence [3] and the absence of Al [26] might stabilize semicrystalline CSH.

Bulk C/S ratios above 0.8 lead to carbonation of the binding agent and formation of scawtite, which decreases compressive strength and increases shrinkage.

4.4. Series with Al-bearing ash: phase formation and physical parameters

The mineralogical investigations of the series with Al-bearing ash show both strongly increasing XRD peak intensities of tobermorite (002) and increasing proportions of SiO_2 soluble in cold HCl. These features may be explained by the effect of Al_2O_3. Decreasing XRD peak intensities for hydrogarnet with increasing bulk C/S ratios, and therefore with increasing additions of Al_2O_3 by the Al-bearing ash, indicate that Al_2O_3 is incorporated in the CSH phases [8,10,31,32]. The formation of tobermorite is favored and the crystallinity within the ab-plane raised [32–34], which reflects the degree of polymerization of the silicate structures. In contrast to the series with lime-sulfate ash, low reactive CaO and the availability of alkalis retards the formation of more highly polymerized silicate structures. Furthermore, high Al content retards the reaction rates at high bulk C/S ratios [30,31,35–39]. Although Al produces tobermorites with high (002) XRD intensities, the retarding effect of Na delays the formation of highly condensed silicate structures.

The drop in strength with increasing bulk C/S ratio correlates with the proportion of SiO_2 insoluble in cold HCl, but not with XRD intensities of tobermorite (002). Decreasing strength with increasing additions of Al-bearing materials (e.g., slag) also were reported elsewhere [1,26,53]. In general, the low compressive strength for series with Al-bearing ash might be related to the low content of free CaO. There, high amounts of ashes are needed to adjust the appropriate bulk C/S ratio (Fig. 1), which may enhance the negative effects of the Al-bearing ash such that highly polymerized silicate structures are not formed.

5. Conclusions

The reference series with commercial lime is characterized by increasing amounts of CSH, well-crystallized tobermorite with increasing bulk C/S ratio, and xonotlite at very high bulk C/S ratios. Using ash from the cellulose industry as a substitute for commercial lime, phase formation in AAC is substantially influenced:

- Ash retards the hydrothermal reaction sequence, and increasing proportions of semicrystalline CSH are not converted into well-crystallized tobermorite.
- Poorly reactive CaO, and elevated alkali and sulfate contents are responsible for the retarding effects of phase formation.
- Highly reactive calcium aluminates in ash produce considerable amounts of hydrogarnet. However, at higher bulk C/S ratios, Al-bearing tobermorite occurs instead of hydrogarnet.
- Al favors high crystallinity parallel to the c-axis, but the retarding effects of the ash inhibits the growth of silicate structures within the ab-plane.
- Scawtite occurs at high bulk C/S ratios where poorly crystallized $CaCO_3$ is present in the ash.

Substitution of lime by ash influences strength such that:

- The highest compressive strengths are obtained by the series with lime-sulfate ash at bulk C/S ratios between 0.7 and 0.8. Thus, this type of ash is favored as a practical substitute for commercial lime.
- Strengths of the AAC series made with Al-bearing ash are markedly lower, which makes this type of ash not applicable in practice.
- The decrease in strength above the optimum C/S ratios is explained by the beginning of decomposition of tobermorite to xonotlite in reference series, and by the formation of scawtite in the series with lime-sulfate ash.

Acknowledgments

This study is funded by the KTI (Komission für Technologie und Innovation, Project no. 2645.2), the participating industrial partners (ZZ Ziegeleien, Hard AG, Keller AG Ziegeleien, Tonwarenfabrik Laufen AG), and the Schweizerische Studiengesellschaft für mineralische Rohstoffe. Information and material was provided by A. Frey (Hard SA, Estavayer-le-Lac) and Cellulose Attisholz AG. This work was directed by Prof. T.J. Peters and his contribution and support are gratefully acknowledged. We also wish to thank an anonymous reviewer for useful comments and suggestions.

References

[1] J. Alexanderson, Cem Concr Res 9 (1979) 507–514.
[2] T. Yamamoto, Ceram Trans 40 (1994) 231–237.
[3] E.S. Al-Wakeel, Einflüsse auf die Phasenbildung und Eigenschaften von Kalksandstein, Thesis, Rheinisch-Westfällische Technische Hochschule, Aachen, 1988.
[4] N. Isu, S. Teramura, K. Ido, T. Mitsuda, Influence of quartz particle size on the chemical and mechanical properties of autoclaved lightweight concrete, in: F.H. Wittman (Ed.), Advances in Autoclaved Aerated Concrete, Balkema, Rotterdam, 1992, pp. 27–34.
[5] N. Isu, H. Ishida, T. Mitsuda, Cem Concr Res 25 (1995) 243–248.
[6] M. Jakob, H. Moertel, Ashes from fluidized bed combustion power plants as a potential raw material for the production of autoclaved aerated concrete, in: F.H. Wittman (Ed.), Advances in Autoclaved Aerated Concrete, Balkema, Rotterdam, 1992, pp. 305–309.
[7] G.L. Kalousek, E.B. Nelson, Cem Concr Res 8 (1978) 283–290.
[8] T. Mumenthaler, T.J. Peters, Vergleichende Untersuchungen über das Verhalten von reinem Quarzsand und einem fluvio-glazialen Sand aus dem schweizerischen Mittelland (Montet, FR) bei der hydrothermalen Härtung von Baustoffen, Schweiz. Geotech. Komm., 1977, p. 45.
[9] T.J. Peters, R. Iberg, T. Mumenthaler, Cem Concr Res 8 (1978) 415–424.
[10] J.L. La Rosa, S. Kwan, M.W. Grutzeck, Ceram Trans 37 (1993) 1–10.
[11] E. Schlegel, Sinterung, Hochtemperaturreaktionen und hydrothermale Reaktionen von CaO und SiO2, Freiberberger Forschungshefte A645, 1982, p. 168.
[12] P. Zgraggen, T.J. Peters, Verwendbarkeit karbonathaltiger Molassesandsteine als Rohstoffe für dampfgehärtete Baustoffe, Schweiz. Geotech. Komm., 1980, p. 59.
[13] C. Buehler, Untersuchungen über die Verwendung karbonatreicher Mergel als Rohstoff für die Herstellung hydrothermal gehärteter Baustoffe., Unpublished Thesis, Universität Bern, Bern, Switzerland, 1986.
[14] A. Raeni, International Symposium on Autoclaved Building Products, Hannover, Germany, 1969.
[15] A. Hauser, Die Verwertung von anorganischen, wenig belasteten Abfallstoffen in hydrothermal gehärteten Baustoffen., Thesis, Universität Bern, Bern, Switzerland, 1996.
[16] S. Aroni, G.J. De Groot, M.J. Robinson, G. Svanholm, F.H. Wittmann, Autoclaved Aerated Concrete: Properties, Testing and Design, Rilem Technical Committees M.C.A., London, E & FN Spon, London, 1993, p. 404.
[17] D. Briesemann, Cem Concr Res 6 (1976) 561–570.
[18] Gundlach, Dampfgehärtete Baustoffe, Bauverlag, Wiesbaden, Berlin, 1973.
[19] G. Svanholm, Influence of water content on properties, in: F.H. Wittman (Ed.), Autoclaved Aerated Concrete—Moisture and Properties, Elsevier, Amsterdam, 1983, pp. 119–130.
[20] S.M. Ickovic, Stroitel'ne Materialy 8 (1962) 36–37.
[21] International Society of Chemical Analysis of Calcareous Materials, 1964, p. 63.
[22] D. Florentin, Annal chemie Analyt Appl 8 (1926) 321–324.
[23] R.S. Boynton, Chemistry and Technology of Lime and Limestone, John Wiley and Sons, Inc., New York, 1980.
[24] T. Mitsuda, K. Sasaki, H. Ishida, J Am Ceram Soc 75 (1992) 1858–1863.
[25] P.P. Budnikow, L.A. Kroitschuk, B.N. Vinogradow, International Conference on Autoclaved Calcium Silicate Building Products, Hannover, 1969.
[26] Z. Sauman, Silikattechnik 24 (1973) 272–278.
[27] E.A. Blakeman, J.A. Gard, C.G. Ramsay, H.F.W. Taylor, J Appl Chem Biotechnol 24 (1974) 239–245.
[28] E.B. Nelson, G.L. Kalousek, Cem Concr Res 7 (1977) 687–694.
[29] S. Sauman, O. Hoffmann, I. Kocuvan, J. Ursic, Silikaty XXV (1981) 289–295.
[30] T. Mitsuda, H.F.W. Taylor, Cem Concr Res 5 (1975) 203–210.
[31] S.A.S. El-Hemaly, T. Mitsuda, H.F.W. Taylor, Cem Concr Res 7 (1977) 429–438.
[32] J.M. Crennan, J.R.L. Dyczek, H.F.W. Taylor, Cem Concr Res 2 (1972) 277–289.
[33] J.R.L. Dyczek, H.W.F. Taylor, Cem Concr Res 1 (1971) 589–605.
[34] H. Stade, W. Wieker, Z Anorg Allg Chem 494 (1982) 179–188.
[35] R.K. Iler, J Colloid Interf Sci 43 (1973) 399–408.
[36] S. Komarneni, R. Roy, D.M. Roy, C.A. Fyfe, G.J. Kennnedy, A.A. Bothner-By, J. Dadok, A.S. Chesnick, J Mater Sci 20 (1985) 4209–4212.
[37] M. Sakiyama, T. Mitsuda, Cem Concr Res 7 (1977) 681–686.
[38] R. Gabrovsek, B. Kurbus, Z. Lengar, Cem Concr Res 16 (1986) 325–332.
[39] R. Gabrovsek, B. Kurbus, D. Mueller, W. Wieker, Cem Concr Res 23 (1993) 321–328.
[40] L. Stevula, J. Petrovic, Silikaty 21 (1977) 331–339.
[41] L. Stevula, J. Petrovic, Cem Concr Res 11 (1981) 549–557.
[42] W. Heugel, T.J. Peters, Internationales Symposium über Die Beziehungen zwischen den Eigenschaften von KS-Produkten und dem Bindemittelaufbau, Karlsruhe, 1978.
[43] G. Frank, Internationales Symposium über Die Beziehungen zwischen den Eigenschaften von KS-Produkten und dem Bindemittelaufbau, Karlsruhe, 1978.
[44] A. Wolter, Tonind Ztg 103 (1979) 772–773.
[45] H. Moertel, K. Piper, Tonind Ztg 102 (1978) 513–518.
[46] J.M. Crennan, S.A.S. El-Hemaly, H.F.W. Taylor, Cem Concr Res 7 (1977) 493–502.
[47] T. Mitsuda, T. Kiribayashi, K. Sasaki, H. Ishida, Influence of hydrothermal processing on the properties of autoclaved aerated concrete, in: F.H. Wittman (Ed.), Advances in Autoclaved Aerated Concrete, Balkema, Rotterdam, 1992, pp. 11–18.
[48] G.E. Bessey, Hydrated calcium silicate products other than hydraulic cements, in: H.F.W. Taylor (Ed.), The Chemistry of Cement, Academic Press, London, 1964, pp. 101–134.
[49] G.L. Kalousek, A.F. Prebus, J Am Ceram Soc 41 (1958) 124–132.
[50] M.W. Grutzeck, A. Benesi, B. Fanning, J Am Ceram Soc 72 (1989) 665–668.
[51] H. Sato, M.W. Grutzeck, Materials Research Society Symposium, Boston, Massachusetts, 1991.
[52] K. Suzuki, T. Nishikawa, H. Ikenaga, S. Ito, Cem Concr Res 16 (1986) 333–340.
[53] G.L. Kalousek, Cem Concr Res 6 (1976) 417–418.